A Game Theoretic Perspective into the Coexistence of WiFi and NR-U at the 6GHz Unlicensed Bands

Aniq Ur Rahman, *Member, IEEE*, Mustafa A. Kishk, *Member, IEEE* and Mohamed-Slim Alouini, *Fellow, IEEE*

arXiv:2012.10644v1 [eess.SY] 19 Dec 2020

Abstract

We study the behaviour of WiFi and 5G cellular networks as they exploit the recently unlocked 6 GHz spectrum for unlicensed access, while conforming to the constraints imposed by the incumbent users. We use tools from stochastic geometry to derive the theoretical performance metrics for users of each radio access technology, which helps us in capturing the aggregate behaviour of the network in a snapshot. We propose a framework where the portions of cellular and WiFi networks are grouped together to form entities. These entities interact to satisfy their Quality of Service demands, by playing a non-cooperative game. The action of an entity corresponds to the fraction of its network elements (WiFi access point and cellular base stations) operating in the 6 GHz band. Due to the decentralized nature of the entities, we find the Nash equilibrium using distributed Best Response Algorithm, where each entity takes actions without any centralized scheduling. The results demonstrate how the system parameters affect the performance of a network at equilibrium and highlight the throughput gains of the networks as a result of using the 6 GHz bands, which offer considerably larger bandwidths. The proposed framework is flexible and can be used to model a variety of scenarios for feasibility and performance assessment of the networks involved.

Index Terms

Coexistence, Spectrum Sharing, Unlicensed, 5G, Game theory

I. INTRODUCTION

Federal Communications Commission (FCC) has recently unlocked the 6 GHz band (from 5.925 GHz to 7.125 GHz) for unlicensed users [1]. This new spectrum band will be used by both WiFi users (Wi-Fi 6E) and cellular users (5G new radio unlicensed or NR-U). In addition, restriction will be applied on unlicensed users to ensure no interference is experienced by the incumbent users [2], which includes fixed point communications such as wireless backhaul [3]. In order to study this new system setup, two types of coexistence needs to be taken into consideration: (i) the coexistence between the unlicensed users and the incumbent users, and (ii) the coexistence between WiFi and 5G users. For the former, as stated earlier, the restrictions deployed by standardization entities will govern the interplay between licensed and unlicensed users. However, such restrictions do not exist for the latter. In particular, WiFi and 5G users, while respecting the aforementioned restrictions, will both try to optimize their system parameters to maximize their Quality of Service (QoS), such as coverage or throughput.

The network is owned by multiple entities [4], where each entity encompasses a portion of the WiFi and a portion of the cellular network. An entity can decide what fraction of its network elements, namely, the WiFi access points (APs) and cellular base stations (BSs), will operate in the unlicensed band. The variation in this fraction affects the performance of the entity's networks. Therefore, the choice of this fraction must be optimal. Moreover, the decision of one entity affects the performance of other entities. This implies that the entities will take a series of decisions, one after the other, and finally settle at a decision which is mutually optimal for all the entities. The interaction of these entities can be modelled as a non-cooperative multi-player game. The performance of the networks of an entity and their respective QoS requirements are used to define the payoff function of that entity.

Conventionally, the users prefer WiFi over cellular connection to access faster and more reliable internet [5], but this behaviour is changing, as the cost of cellular internet is decreasing, thereby incentivizing its use over WiFi [6]. Moreover cellular base stations cover a larger area compared to WiFi access points, which means that handovers are not that frequent, even for mobile users like vehicles and aerial drones. These differences in the use cases hint at the coexistence of these technologies instead of one taking over the other. The convergence between WiFi and 5G will open new business avenues and ultimately improve the user experience [7], as the two radio access technologies (RATs) will simultaneously complement each other while competing for the available bandwidth [6]. Therefore, improvement in the performance of both RATs is essential for transitioning into the future smoothly.

A. Related Works

1) Coexistence in the Unlicensed Spectra: Recent surveys [5], [8], have reviewed the coexistence of WiFi and cellular networks in the 6 GHz unlicensed bands, and provided an extensive list of relevant literature. Fair coexistence of LTE with WiFi has been extensively studied for the 5 GHz band [9]. In [10], the authors define fairness in terms of datarate. Proportional fairness demonstrated in [11], allows each RAT to access the unlicensed channel for equal amount of time, which is better in

Aniq Ur Rahman, Mustafa A. Kishk and Mohamed-Slim Alouini are with King Abdullah University of Science and Technology (KAUST), CEMSE division, Thuwal 23955-6900, Saudi Arabia (e-mail: aniqur.rahman@kaust.edu.sa; mustafa.kishk@kaust.edu.sa; slim.alouini@kaust.edu.sa). This work was funded in part by the Center of Excellence for NEOM Research at KAUST.

contrast to the notion of fairness championed by 3GPP. Recently, coexistence of 5G NR with WiFi is also being investigated in the 60 GHz mmWave band [12].

2) Stochastic Geometry for Studying Coexistence: Authors in [13] make use of tools from stochastic geometry to study the coexistence of narrow band (NB) and ultra-wide band (UWB) wireless nodes. In [14], the authors analyse the performance of an LTE-WiFi network coexisting in the unlicensed 5 GHz band using stochastic geometry. The study however was purely dependent on simulations and did not provide theoretical expressions for the performance metrics.

3) Spectrum Sharing using Game Theory: Spectrum sharing is of key significance in alleviating mutual interference and it allows multiple users to utilize the spectrum in parallel [15]. The cognitive radio literature [16], [17], [18], [19] treats the open spectrum sharing problem as a game, where the secondary users compete for the unlicensed spectrum. The users' actions include varying certain parameters such as transmission power, access duration and modulation technique. The payoff is generally modelled as a function of the experienced quality of service, such as throughput or latency.

B. Contributions

The major contributions of our work are as follows:

- We study the behaviour of WiFi and 5G cellular networks as they utilize the unlicensed 6 GHz spectrum, while respecting the constraints imposed by the incumbent users. We use tools from stochastic geometry to derive the coverage probabilities and average datarate for users of each radio access technology. This helps us captures the aggregate behaviour of the network in a snapshot and define the performance metrics theoretically.
- The set of all network elements (WiFi APs and 5G BSs) is split into multiple disjoint sets, referred to as entities. Next, we define a framework where these entities interact to satisfy their QoS demands, by playing a non-cooperative game. The actions denote the fraction of network elements (WiFi APs and cellular BSs) in each entity, operating in 6 GHz.
- Due to the distributed nature of the game, we find the Nash equilibrium using distributed Best Response Algorithm, where each entity takes actions without any time synchronization or scheduling.
- The simulation parameters used in this study are taken from real-world network deployments. For example, we have considered the 5G base station deployment to match Shanghai's Hongqiao district's 5G network.
- The framework developed in this study is highly flexible and can be used to analyze a variety of scenarios, across various unlicensed bands.

The rest of the paper is organized as follows. In Sec. 2 we describe the system model and then develop a mathematical understanding of the performance metrics in the next section, Sec. 3. In Sec. 4 we propose a game theoretic framework to study the problem, and show the results in Sec. 5. The paper is finally concluded in Sec. 6.

II. SYSTEM MODEL

We consider a system where three coexisting wireless networks are utilizing the 6-GHz band: (i) the WiFi network consisting of the APs and the WiFi users, (ii) the cellular network consisting of cellular BSs and its users, and (iii) a network of the incumbent users, utilizing the 6-GHz band licensed to them for fixed point backhaul operation. We consider this to be the primary usage of this band and the performance of the first two networks should not hamper the experience of the incumbent users. To enforce this, each of these incumbent users have an *exclusion zone* around them, within which the 6-GHz band cannot be used by the WiFi and cellular networks [1].

The WiFi APs and Cellular BSs are divided among various *entities*, i.e., parts of the network are owned by different mobile operators. The entities control their own utilization of the unlicensed spectrum to maximize their datarate in response to the 6-GHz spectrum utilization by the other entities. The interaction between the entities is modelled as a non-cooperative game. The system is illustrated in Fig. 1 and a sample network deployment scenario is presented in Fig. 2.

A. Network Deployment

1) Incumbent Users: We populate the $\mathbb{R}^2$ plane with incumbent users, which follow a homogeneous Poisson point process (PPP) Φ_z with parameter λ_z. Around each of these incumbent users, we have an exclusion zone of radius ρ. The set of all the exclusion zones is described mathematically as: $\Xi_\rho = \bigcup_{\mathbf{x}\in\Phi_z} b(\mathbf{x},\rho)$, where $b(\mathbf{x},\rho)$ denotes a disk of radius ρ centred at point $\mathbf{x}$.

2) WiFi Network: Now we deploy the WiFi access points (APs) as a homogeneous PPP Φ_w of intensity λ_w. The set of APs which are allowed to use the unlicensed spectrum lie outside the exclusion zones Ξ_ρ and can be carved out as a Poisson Hole Process (PHP) from Φ_w. We define this PHP as $\hat{\Phi}_w \triangleq \Phi_w \setminus \Xi_\rho$.

Approximation 1. *The PHP $\hat{\Phi}_w$ can be approximated as a uniform PPP of intensity $\bar{\lambda}_w = \lambda_w \exp(-\pi\lambda_z\rho^2)$, see [20], [21].*

A fraction $\delta_w \in [0,1]$ of APs in $\hat{\Phi}_w$ operate in the unlicensed band. Therefore, we can write: $\Phi_w = \Phi_{w|L} \bigcup \Phi_{w|U}$, where $\Phi_{w|L}$ is the set of APs operating in their licensed 2.4GHz WiFi band, and $\Phi_{w|U}$ is set of APs using the unlicensed 6GHz

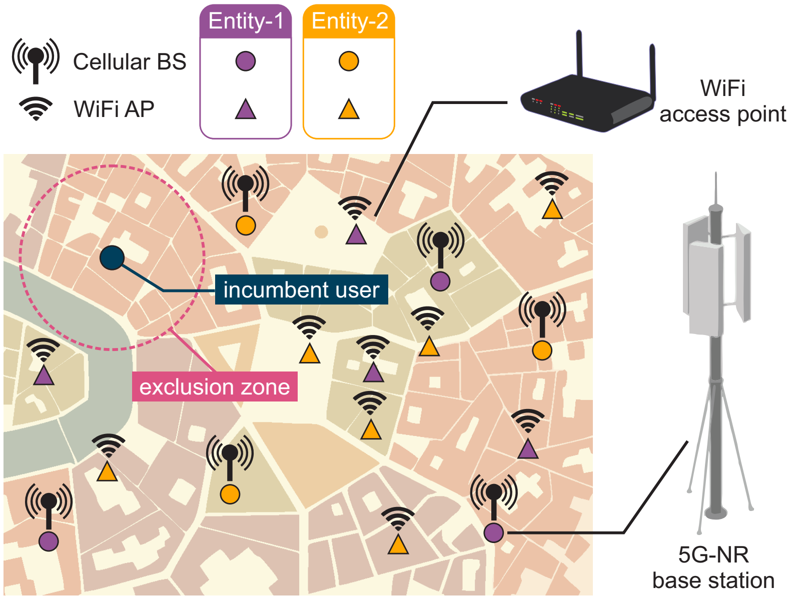

Fig. 1: System Illustration.

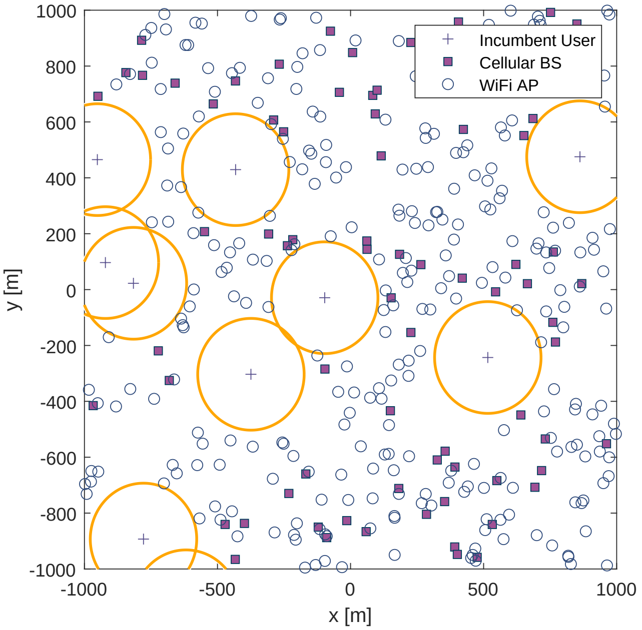

Fig. 2: Sample network deployment showing $\Phi_z, \Xi_\rho, \hat{\Phi}_c, \hat{\Phi}_w$. The exclusion zones of radius ρ are drawn around the incumbent users as yellow circles. Parameters: $\lambda_z = 1$ user/km^2, $\lambda_c = 25$ BS/km^2, $\lambda_w = 100$ AP/km^2, $\rho = 200$ m.

band. Furthermore, we can approximate $\Phi_{w|L}$ and $\Phi_{w|U}$ as independent homogeneous PPPs, such that: $\Phi_{w|U} \triangleq \mathrm{PPP}(\delta_w \bar{\lambda}_w)$, and $\Phi_{w|L} \triangleq \mathrm{PPP}(\lambda_w - \delta_w \bar{\lambda}_w)$, where $\mathrm{PPP}(\Lambda)$ denotes a homogeneous Poisson point process having intensity Λ.

The WiFi users form a cluster point process, where each cluster has a radius ρ_w, and is centred around an AP. The WiFi users are denoted as Ψ_w and described as: $\Psi_w = \bigcup_{\mathbf{x} \in \Phi_w} \psi_{\mathbf{x}} + \mathbf{x}$, where $\psi_{\mathbf{x}}$ is a Matérn cluster centred around $\mathbf{x}$. In a Matérn cluster, the distance between a point in the cluster to the center follows a triangular distribution bounded within $(0, \rho_w)$, see [22].

3) Cellular Network: Similar to the deployment of the WiFi APs, we model the set of cellular Base stations as an independent homogeneous PPP Φ_c of intensity λ_c, such that only the BSs lying outside the exclusion zones are permitted to utilize the unlicensed 6-GHz spectrum. The set of BSs outside the exclusion zones is a PHP $\hat{\Phi}_c = \Phi_c \setminus \Xi_\rho$ and a fraction $\delta_c \in [0, 1]$ of BSs in $\hat{\Phi}_c$ operate in the unlicensed band.

Approximation 2. *The PHP* $\hat{\Phi}_c$ *is approximated as a homogeneous PPP with intensity* $\bar{\lambda}_c = \lambda_c \exp(-\pi\lambda_z\rho^2)$*, see [20], [21].*

Alternatively, Φ_c can be described as: $\Phi_c = \Phi_{c|L} \bigcup \Phi_{c|U}$, where $\Phi_{c|L} \triangleq \mathrm{PPP}(\lambda_c - \delta_c\bar{\lambda}_c)$ and $\Phi_{c|U} \triangleq \mathrm{PPP}(\delta_c\bar{\lambda}_c)$ operate in the licensed and unlicensed bands, respectively. Furthermore, the cellular users are spread in $\mathbb{R}^2$ as an independent homogeneous PPP.

The transmit powers of the cellular BSs, WiFi APs and incumbent users are p_c, p_w and p_z respectively. The bandwidth offered by the unlicensed 6-GHz band is B_U. The bandwidths of the cellular and WiFi networks operating in their corresponding licensed bands is denoted as $B_{c|L}$ and $B_{w|L}$, respectively. We also denote the bandwidths of the cellular and WiFi users in the unlicensed band as $B_{c|U}$ and $B_{w|U}$ respectively, and both are equal to B_U in value.

B. Downlink Interference

Definition 1. *The user at the origin receives a signal of strength* $\xi(\mathbf{x})$ *from the transmitting node at* $\mathbf{x}$*:* $\xi(\mathbf{x}) = p_{\mathbf{x}}H\|\mathbf{x}\|^{-\alpha}$*, where* $p_{\mathbf{x}}$ *is the transmit power of the node* $\mathbf{x}$ *and* $H \sim \exp(1)$ *is the random variable signifying Rayleigh fading and* α *is the path-loss coefficient.*

In *unlicensed access*, the typical user experiences interference from all the networks utilizing the unlicensed 6-GHz spectrum, namely, Φ_z, $\Phi_{c|U}$ and $\Phi_{w|U}$. We define this set as $\Phi^U \triangleq \Phi_z \cup \Phi_{c|U} \cup \Phi_{w|U}$. The interference to cellular and WiFi users in unlicensed access is denoted as $I_{c|U}$ and $I_{w|U}$, respectively, and defined as follows:

$$I_{c|U} \triangleq \sum_{\mathbf{x}\in\Phi^U\setminus\{\mathbf{x}_0\}} \xi(\mathbf{x}), \qquad \mathbf{x}_0 = \arg\min_{\mathbf{x}\in\Phi_{c|U}} \|\mathbf{x}\|, \tag{1}$$

$$I_{w|U} \triangleq \sum_{\mathbf{x}\in\Phi^U\setminus\{\mathbf{x}_0\}} \xi(\mathbf{x}), \qquad \mathbf{x}_0 \sim \{\mathbf{x} \in \Phi_{w|U} : \|\mathbf{x}\| < \rho_w\}. \tag{2}$$

In *licensed access*, the typical user experiences interference from its own network. The cellular and WiFi users receive interference from the nodes in $\Phi_{c|L}$ and $\Phi_{w|L}$ respectively. The interference to cellular and WiFi users in licensed access is denoted as $I_{c|L}$ and $I_{w|L}$ respectively, and defined as follows:

$$I_{c|L} \triangleq \sum_{\mathbf{x}\in\Phi_{c|L}\setminus\{\mathbf{x}_0\}} \xi(\mathbf{x}), \qquad \mathbf{x}_0 = \arg\min_{\mathbf{x}\in\Phi_{c|L}} \|\mathbf{x}\|, \tag{3}$$

$$I_{w|L} \triangleq \sum_{\mathbf{x}\in\Phi_{w|L}\setminus\{\mathbf{x}_0\}} \xi(\mathbf{x}), \qquad \mathbf{x}_0 \sim \{\mathbf{x} \in \Phi_{w|L} : \|\mathbf{x}\| < \rho_w\}. \tag{4}$$

It must be noted that unlike the cellular users, the WiFi users do not connect to the nearest access point. Instead, they are connected to any single AP via closed-access while being within its range. This is expressed mathematically in equations (2) and (4) as $\mathbf{x}_0 \sim \{\mathbf{x} \in \Phi_{w|M} : \|\mathbf{x}\| < \rho_w\}$, $M \in \{U, L\}$, where $\mathbf{x}_0$ is the access point, to which the WiFi user connects. Next, we define the signal-to-interference-plus-noise ratio (SINR), which is ultimately used for the downlink analysis in the upcoming section.

Definition 2. *The signal-to-interference-plus-noise ratio for a typical user is defined as:* $\mathrm{SINR}_{k|M} \triangleq \dfrac{\xi(\mathbf{x}_0)}{\sigma_k^2 + I_{k|M}}; k \in \{c, w\}, M \in \{U, L\}$*, where* σ_c^2 *and* σ_w^2 *are the receiver noise power for the cellular and WiFi users respectively.*

C. Multi-Entity Competition

It is seen in [4] that Mobile Virtual Network Operators (MVNOs) which are a conglomeration of multiple Mobile Network Operators (MNOs) generate more revenue compared to multiple MNOs operating independently. Therefore, we can envision an MVNO having both RATs under its umbrella, which then allocates the resources judiciously in order to achieve the best overall performance.

We begin by defining a set of entities, $\mathsf{e}_i \in \mathcal{E}$ which consists of a cellular network and a WiFi network. Entity e_i's share of the cellular network is v_c^i and its share of WiFi network is v_w^i, such that, $\sum_{\mathsf{e}_j\in\mathcal{E}} v_c^j = 1$, and $\sum_{\mathsf{e}_j\in\mathcal{E}} v_w^j = 1$. The network of type $k \in \{c, w\}$ owned by entity e_i is denoted as $\Phi_k^i \triangleq \mathrm{PPP}(v_k^i\,\lambda_k)$. The portion of Φ_k^i which lies outside the exclusion zones is denoted as $\hat{\Phi}_k^i \triangleq \mathrm{PPP}(v_k^i\,\bar{\lambda}_k)$. A fraction δ_c^i of the cellular base stations $\in \hat{\Phi}_c^i$ and a fraction δ_w^i of the WiFi APs $\in \hat{\Phi}_w^i$ operate in the unlicensed 6-GHz band. The fraction of network elements in Φ_k^i which operate in the licensed and unlicensed bands are denoted as $\Phi_{k|L}^i \triangleq \mathrm{PPP}(\delta_k^i\,v_k^i\,\bar{\lambda}_k)$, and $\Phi_{k|U}^i \triangleq \mathrm{PPP}(v_k^i\,\lambda_k - \delta_k^i\,v_k^i\,\bar{\lambda}_k)$, respectively. Moreover, each entity has its own QoS requirement in the form of minimum datarates for its WiFi and cellular networks. The minimum datarate requirements of e_i for the cellular and WiFi networks are denoted as $\hat{\sigma}_c^i$ and $\hat{\sigma}_w^i$, respectively. The concept of entities is illustrated in Fig. 3. Finally, we present a formal definition for an entity as follows:

Definition 3. *An entity* $\mathsf{e}_i \in \mathcal{E}$ *can be defined by the tuple* $\left(v_c^i, v_w^i, \delta_c^i, \delta_w^i, \hat{\sigma}_c^i, \hat{\sigma}_w^i\right)$*, with the following description:*

- v_c^i *is the cellular network share,*
- v_w^i *is the WiFi network share,*

- *δ_c^i is the cellular unlicensed spectrum utilization,*
- *δ_w^i is the WiFi unlicensed spectrum utilization,*
- *$\hat{\sigma}_c^i$ is the cellular datarate threshold,*
- *$\hat{\sigma}_w^i$ is the WiFi datarate threshold.*

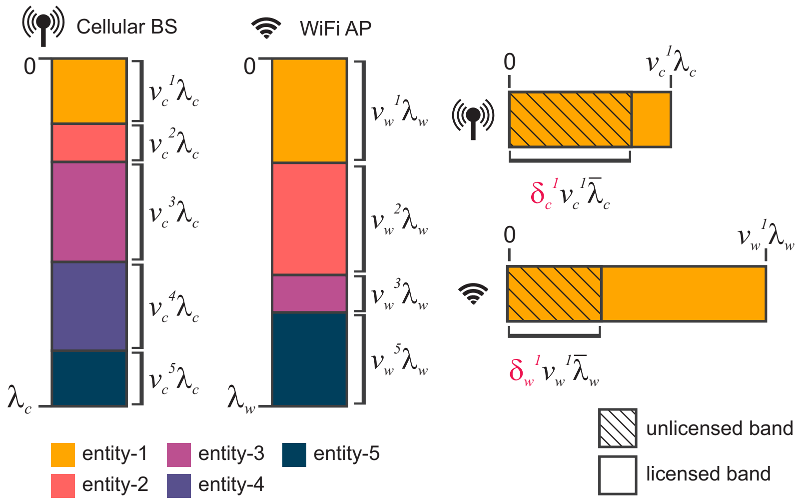

Fig. 3: Division of the network among a set of Entities.

In this model, $v_c^i = 0$ implies that the entity lacks a cellular network and $v_w^i = 0$ denotes the absence of a WiFi network. In the context of the entire network, the fraction denoting the utilization of the unlicensed band by the cellular and WiFi networks is defined as $\delta_c \triangleq \sum_{e_j \in \mathcal{E}} v_c^j \delta_c^j$ and $\delta_w \triangleq \sum_{e_j \in \mathcal{E}} v_w^j \delta_w^j$ respectively.

III. PERFORMANCE METRICS

In this section we derive the performance metrics, which are used to define the payoff function in the Game Theoretic formulations in the next section.

A. *Coverage Probability*

We begin by presenting the theoretical expressions of coverage probability for the cellular and WiFi networks operating in the licensed and unlicensed bands based on the parameters discussed in Sec. II. Formally, we define the coverage probability as follows:

Definition 4. *Coverage Probability is defined as the probability that the SINR experienced by a user is above the threshold value of γ, i.e., $P_{k|M} \triangleq \mathbb{P}\left(\mathrm{SINR}_{k|M} > \gamma\right)$, where $k \in \{c, w\}$ denotes the network (cellular/WiFi), and $M \in \{U, L\}$ denotes the mode of access (unlicensed/licensed).*

1) Cellular Users: The coverage probability for cellular users operating in the licensed and unlicensed bands are described in Lemma 1 and Lemma 2 respectively, as follows.

Lemma 1. *The coverage probability for a cellular user operating in the licensed cellular band is:*

$$P_{c|L}(\gamma, \delta_c) = 2\pi\left(\lambda_c - \delta_c \bar{\lambda}_c\right) \int_0^\infty \exp\left\{ -\frac{\sigma_c^2 \gamma}{p_c} r^\alpha - \pi\left(\lambda_c - \delta_c \bar{\lambda}_c\right)\left(1 + \zeta(\gamma, \alpha)\right) r^2 \right\} r\, dr, \tag{5}$$

where $\zeta(\gamma, \alpha) = \frac{\gamma^{\frac{2}{\alpha}}}{2} \int_{\gamma^{-\frac{2}{\alpha}}}^\infty \frac{1}{1 + x^{\frac{\alpha}{2}}}\, dx$.

Proof. The proof is provided in [23, Proposition 5.2.3] and is hence skipped. ☐

Lemma 2. *The coverage probability for a cellular user operating in the unlicensed 6-GHz band is: $P_{c|U}(\gamma, \delta_c, \delta_w) =$*

$$2\pi\delta_c \bar{\lambda}_c \int_0^\infty \exp\left\{ -\frac{\sigma_c^2 \gamma}{p_c} r^\alpha - \left(\frac{\pi \gamma^{2/\alpha}}{p_c^{2/\alpha} \mathrm{sinc}\left(\frac{2}{\alpha}\right)} \left(\delta_w \bar{\lambda}_w p_w^{\frac{2}{\alpha}} + \lambda_z p_z^{\frac{2}{\alpha}}\right) + \pi \delta_c \bar{\lambda}_c \left(1 + \zeta(\gamma, \alpha)\right) \right) r^2 \right\} r\, dr, \tag{6}$$

where $\zeta(\gamma, \alpha) = \frac{\gamma^{\frac{2}{\alpha}}}{2} \int_{\gamma^{-\frac{2}{\alpha}}}^\infty \frac{1}{1 + x^{\frac{\alpha}{2}}}\, dx$.

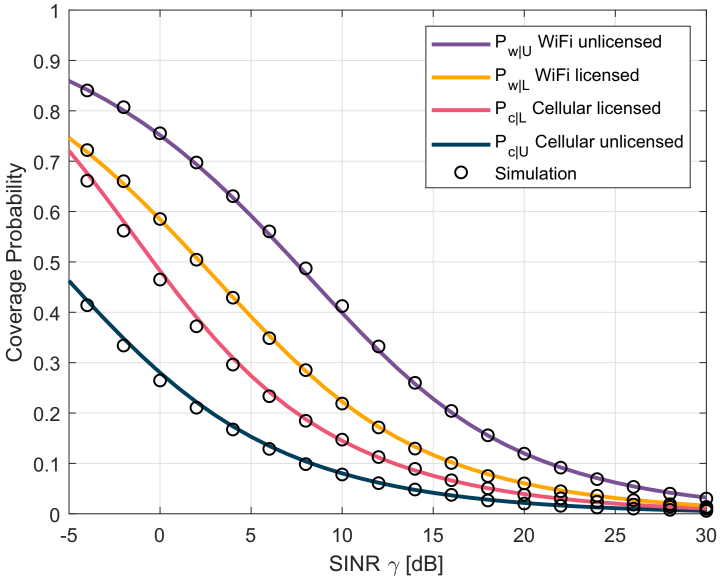

Fig. 4: Coverage probability for the cellular and WiFi users operating in the licensed and unlicensed spectra. $\lambda_z = 1\ \text{user/km}^2$, $\lambda_c = 25\ \text{BS/km}^2$, $\lambda_w = 100\ \text{AP/km}^2$, $\rho = 200$ m, $\rho_w = 50$ m, $p_z = 1$ W, $p_c = 2$ W, $p_w = 1$ W, $\delta_c = 0.7$, $\delta_w = 0.2$.

Proof. Using the definition of SINR and coverage probability above, we express the coverage probability for a cellular user operating in the unlicensed band as: $P_{c|U}(\gamma, \delta_c, \delta_w) = \mathbb{P}\left(\frac{p_c H R^{-\alpha}}{\sigma_c^2 + I_{c|U}} > \gamma\right)$. Then we take the expectation over the two random quantities: the distance between the cellular user and its base station R, and the interference $I_{c|U}$. The distance R follows the distribution:

$$f_R^c(r) = 2\pi\delta_c\bar{\lambda}_c r\ \exp(-\pi\delta_c\bar{\lambda}_c r^2), \quad r \geq 0.$$

Further, exploiting the CDF of H which is exponentially distributed as $H \sim \exp(1)$, we arrive at:

$$P_{c|U} = \int_0^\infty e^{-\sigma_c^2 p_c^{-1}\gamma r^\alpha} \times \prod_{j\in\{w,z,c\}} \mathcal{L}_{c,j|U}\left(\frac{r^\alpha\gamma}{p_c}\right) \times f_R^c(r)\,dr,$$

where $\mathcal{L}_{c,j|U}(s)$ is the Laplace transform of the interference experienced by the cellular users in the unlicensed band from transmitters of type $j \in \{c, w, z\}$. Plugging the expression for the Laplace transforms from the Appendix yields the final equation. □

2) WiFi Users: The coverage probability for WiFi users operating in the licensed and unlicensed bands are described in Lemma 3 and Lemma 4 respectively, as follows.

Lemma 3. *The coverage probability for a WiFi user operating in the licensed WiFi band is:* $P_{w|L}(\gamma, \delta_w) =$

$$\frac{2}{\rho_w^2}\int_0^{\rho_w} \exp\left\{-\frac{\sigma_w^2\gamma}{p_w}r^\alpha - \frac{\pi\gamma^{2/\alpha}\left(\lambda_w - \delta_w\bar{\lambda}_w\right)}{\operatorname{sinc}\left(\frac{2}{\alpha}\right)}r^2\right\} r\,dr. \tag{7}$$

Proof. The proof is provided in [23, Proposition 5.2.1] and is hence skipped. □

Lemma 4. *The coverage probability for a WiFi user operating in the unlicensed 6-GHz band is:* $P_{w|U}(\gamma, \delta_c, \delta_w) =$

$$\frac{2}{\rho_w^2}\int_0^{\rho_w} \exp\left\{-\frac{\sigma_w^2\gamma}{p_w}r^\alpha - \frac{\pi\gamma^{2/\alpha}}{p_w^{2/\alpha}\operatorname{sinc}\left(\frac{2}{\alpha}\right)}\left(\delta_w\bar{\lambda}_w p_w^{\frac{2}{\alpha}} + \delta_c\bar{\lambda}_c p_c^{\frac{2}{\alpha}} + \lambda_z p_z^{\frac{2}{\alpha}}\right)r^2\right\} r\,dr. \tag{8}$$

Proof. The proof can be sketched on the same lines as shown in the proof of Lemma 2. Here, the distance R between a WiFi user and the access point it is associated with, follows the distribution: $f_R^w(r) = \frac{2r}{\rho_w^2} \cdot 1\{0 \leq r < \rho_w\}$. □

In Fig. 4, we see that our theoretical expressions for coverage probability described in Lemmas 1-4, are in agreement with the Monte Carlo simulation results.

B. Average Datarate

In this section, we define the average datarate of typical cellular and WiFi users. Formally, it is defined as the average of the datarates experienced by the users associated with the network elements of an entity, either cellular or WiFi. In the following two theorems, we present theoretical expressions for the average datarate of the cellular and WiFi users, derived using Stochastic Geometry.

Theorem 1. *The average datarate of a user served by the cellular network of entity* $\mathbb{e}_i$ *is:*

$$\sigma_c^i(\gamma,\delta_c,\delta_w,\delta_c^i) = B_{c|U}\log_2\left(1+\gamma\right)P_{c|U}(\gamma,\delta_c,\delta_w)\cdot\frac{\delta_c^i\bar{\lambda}_c}{\lambda_c} + B_{c|L}\log_2\left(1+\gamma\right)P_{c|L}(\gamma,\delta_c)\cdot\left(1-\frac{\delta_c^i\bar{\lambda}_c}{\lambda_c}\right). \tag{9}$$

Proof. We can express the time-averaged datarate of a cellular user associated with a base station $\mathbf{x}\in\Phi_c^i$ of entity $\mathbb{e}_i$ as: $B_{\mathbf{x}}\log_2(1+\gamma)\,\mathbb{P}(\mathrm{SINR}_{\mathbf{x}}>\gamma)$, where $B_{\mathbf{x}}$ is the bandwidth offered by $\mathbf{x}$. Taking expectation over Φ_c^i, we get:

$$\begin{aligned}\sigma_c^i &\overset{(a)}{=} \sum_{M\in\{U,L\}}\mathbb{E}_{\Phi^i_{c|M}}\Big[B_{\mathbf{x}}\log_2(1+\gamma)\,\mathbb{P}(\mathrm{SINR}_{\mathbf{x}}>\gamma)\Big]\\ &\overset{(b)}{=} \sum_{M\in\{U,L\}}\frac{|\Phi^i_{c|M}|}{|\Phi^i_c|}\,B_{c|M}\log_2(1+\gamma)\,P_{c|M}\end{aligned}$$

Step (a) follows from $\Phi_c^i=\Phi^i_{c|U}\cup\Phi^i_{c|L}$. In step (b), $|\Phi|$ denotes the intensity of a PPP Φ. □

Theorem 2. *The average datarate of a user served by the WiFi network of entity* $\mathbb{e}_i$ *is:*

$$\sigma_w^i(\gamma,\delta_c,\delta_w,\delta_w^i) = B_{w|U}\log_2\left(1+\gamma\right)P_{w|U}(\gamma,\delta_c,\delta_w)\cdot\frac{\delta_w^i\bar{\lambda}_w}{\lambda_w} + B_{w|L}\log_2\left(1+\gamma\right)P_{w|L}(\gamma,\delta_w)\cdot\left(1-\frac{\delta_w^i\bar{\lambda}_w}{\lambda_w}\right). \tag{10}$$

Proof. The proof can be sketched on the same lines as Theorem 1, and is hence skipped. □

In Fig. 5, we present the average cellular and WiFi datarates for various values of δ_c and δ_w. The cellular datarate peaks at $\delta_c=1$ and $\delta_w=0$ implying that it performs the best in the absence of interference from the WiFi network in the unlicensed band. Moreover, for any value of δ_w, the maximum cellular datarate is observed at $\delta_c=1$. However, the WiFi datarate has a maximum at $\delta_w\approx0.7$ for any value of δ_c indicating that it performs best when the self-interference in the unlicensed band by the WiFi network is kept under check. In other words, if all the WiFi APs operate in the unlicensed band, the interference increases and aggravates the datarate. This suggests that the WiFi networks should under-utilize the 6-GHz spectrum for best results.

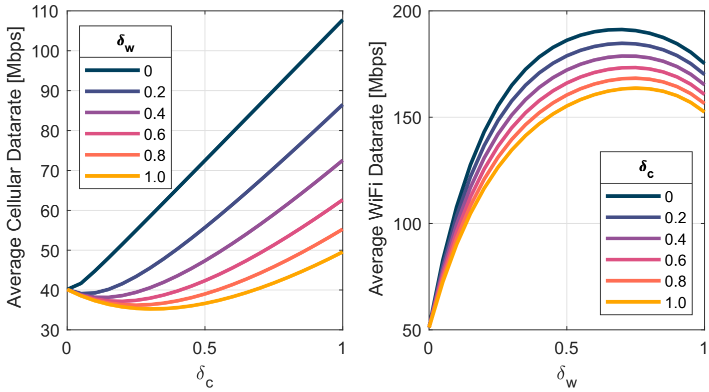

Fig. 5: Average cellular and WiFi datarates. Parameters: $|\mathcal{E}|=1$, $\lambda_z=1$ user/km^2, $\lambda_c=25$ BS/km^2, $\lambda_w=100$ AP/km^2, $\rho=200$ m, $\rho_w=50$ m, $p_z=1$ W, $p_c=2$ W, $p_w=1$ W, $B_U=240$ MHz, $B_{c|L}=80$ MHz, $B_{w|L}=80$ MHz, $\gamma=10$ dB.

In the next section, we invoke the concept of non-cooperative games to model the interaction between different entities, where each entity tries to maximize the value of its payoff function by taking the necessary action.

IV. GAME FORMULATION

Each entity $\mathtt{e}_i$ adjusts its unlicensed spectrum utilization δ_c^i, δ_w^i to maximize its own payoff function. The interaction of all the entities can be modelled as a non-cooperative game. From the perspective of entity $\mathtt{e}_i$, the tuple (δ_c^i, δ_w^i) is the action. Therefore we represent the action of $\mathtt{e}_i$ as the vector:

$$\mathbf{a}_i \triangleq \begin{bmatrix} \delta_c^i \\ \delta_w^i \end{bmatrix} \in [0,1]^2. \tag{11}$$

The set of actions of all the entities except $\mathtt{e}_i$ is denoted as:

$$\mathcal{A}_{-i} \triangleq \left\{ \forall \mathtt{e}_j \in \mathcal{E} \setminus \{\mathtt{e}_i\} : \mathbf{a}_j \right\}. \tag{12}$$

Definition 5. *The payoff function of entity* $\mathtt{e}_i$ *is defined as* $f_i(\mathbf{a}_i, \mathcal{A}_{-i}) : [0,1]^{2|\mathcal{E}|} \mapsto \mathbb{R}$*, which maps the actions of all the entities to a real value.*

Definition 6. *The game is defined as* $\mathfrak{G}(\mathcal{E}, \mathcal{A}, \mathcal{F})$*, where entities* $\mathcal{E}$ *are the players,* $\mathcal{A} \triangleq [0,1]^{2|\mathcal{E}|}$ *is the action profile and* $\mathcal{F} \triangleq \left(f_i, \cdots f_{|\mathcal{E}|}\right)$ *is the set of payoff functions of all players.*

In this non-cooperative framework, we impose a strict condition that the entities are not aware of the actions of other entities. When an entity takes an action, it is based on the observations from the environment and the action then alters the environment. Each network element of an entity can measure the power of the interfering signals in the licensed and unlicensed bands, and leverage this information to estimate the average datarate experienced by the users in its proximity.

Since there is no coordination among the entities, we cannot schedule the decision making process as a round-robin sequence. Instead we equip each entity with an independent Poisson clock [24] with the same rate, which triggers the entity to take an action (see Fig. 6). We also assume that the time taken by each entity to choose an action is small enough to minimize the probability of more than one entity acting simultaneously.

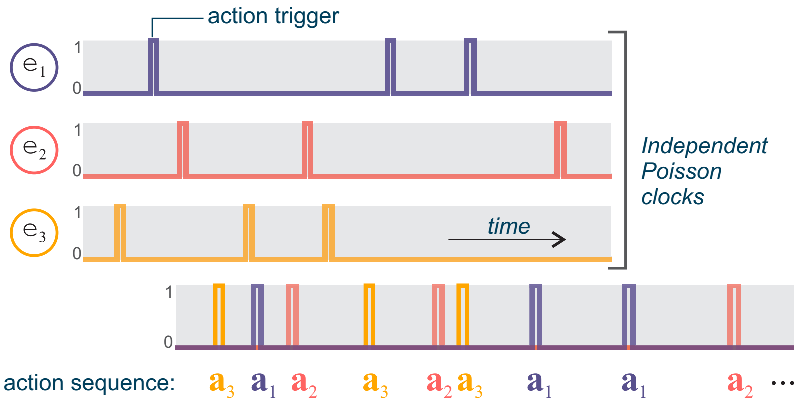

Fig. 6: Action sequence as a result of independent Poisson clocks.

Approximation 3. *The action sequence generated as a consequence of each entity being triggered by its Poisson clock is approximated as a sequence where each element is the action of an entity drawn from the set of all entities with uniform probability.*

Algorithm 1 Distributed Best Response Algorithm

```
1: $\mathbf{a}_j \sim [0,1]^2; \quad \forall \mathtt{e}_j \in \mathcal{E}$                    ▷ Initialization
2: $n_j \leftarrow 0; \quad \forall \mathtt{e}_j \in \mathcal{E}$
3: while True do
4:     $i \sim \text{uniform}(1, |\mathcal{E}|)$                                  ▷ Approximation 3
5:     $\mathbf{a}_i \leftarrow \arg\max_{\mathbf{a} \in [0,1]^2} f_i(\mathbf{a}, \mathcal{A}_{-i})$          ▷ Best Response
6:     $n_i \leftarrow n_i + 1$
7:     $\mathbf{A}_i^{[n_i]} \leftarrow \mathbf{a}_i$                                     ▷ Update action vector
8: end while
```

The action vector of entity $\mathtt{e}_i$ at the m^{th} update is denoted as $\mathbf{A}_i^{[m]}$. For a system-level implementation, the steps 2, 6 and 7 are redundant. However, we include them for convergence analysis, in order to understand how quickly the entities reach Nash equilibrium. The Nash equilibrium of the game described above, is formally defined as follows.

Definition 7. *The Nash equilibrium is defined as the matrix of action vectors of all the entities* $\mathbf{Q} \triangleq \left[\mathbf{a}_1 \cdots \mathbf{a}_m \cdots \mathbf{a}_{|\mathcal{E}|}\right]$ *such that the action vector of each entity remains unchanged in their latest iterations, i.e.,*

$$\sum_{e_j \in \mathcal{E}} \left\| \mathbf{A}_j^{[n_j]} - \mathbf{A}_j^{[n_j-1]} \right\| = 0. \tag{13}$$

A. *Payoff Function*

Next, we mathematically define the payoff function which the entities can adopt to find their best response. The condition that the cellular and WiFi datarates are greater than the minimum values, can be indicated as $1_{\sigma_i} \triangleq 1\left\{\bigcap_{k\in\{c,w\}} \left(\sigma_k^i \geq \hat{\sigma}_k^i | v_k^i > 0\right)\right\}$. The *preference* for the cellular and WiFi networks in an entity $\mathbb{e}_i$ is translated by the weights $\theta_c^i > 0$ and $\theta_w^i > 0$ respectively, which are used in the definition of the payoff function below.

$$f_i \triangleq 1_{\sigma_i} \times \sum_{k\in\{c,w\}} \theta_k^i \sigma_k^i 1\{v_k^i > 0\}. \tag{14}$$

This ensures that the action which fulfils the minimum datarate will always be chosen in the presence of actions which might have a higher weighted sum of datarates but do not meet the datarate requirements for both networks simultaneously.

V. RESULTS & DISCUSSION

We present the results for the interaction between the entities and analyse how the various parameters affect the datarate achieved by the entities at equilibrium, in order to provide useful design insights for implementation. The range of the parameters used in the system model are summarized in Table I. For all the results that follow, we use the following values: $\lambda_z = 1$ user/km^2, $\lambda_c = 25$ BS/km^2, $\lambda_w = 100$ AP/km^2, $\rho = 200$ m, $\rho_w = 50$ m, $p_z = 1$ W, $p_c = 2$ W, $p_w = 1$ W, $B_U = 240$ MHz, $B_{c|L} = 80$ MHz, $B_{w|L} = 80$ MHz, $\gamma = 10$ dB

TABLE I: Range of System Parameters

Parameter	**Values**	**Source**
B_U	$\in$ [40, 80, 160, 240, 320] MHz	[8], [5]
$B_{c\|L}$	$\in$ [20, 40, 80, 100] MHz	[25]
$B_{w\|L}$	$\in$ [20, 40, 80, 160] MHz	[26]
p_z	$\leq$ 30 dBm	[8]
p_c	$\leq$ 36 dBm	[8]
p_w	$\leq$ 36 dBm	[8]
λ_z	1 km^{-2}	[27]
λ_c	$\in$ [25, 50, 250] km^{-2}	[28], [29]
λ_w	$\in$ [100, 400] km^{-2}	[30]
ρ	200 m	
ρ_w	50 m	[31]

A. *Effect of Network Preference*

We define two entities, each demanding a minimum cellular datarate of 30 Mbps and minimum WiFi datarate of 100 Mbps. To visualize the behaviour of the payoff function, we vary the ratio $\frac{\theta_c^i}{\theta_w^i}$ and plot the values of cellular and WiFi datarates summarized for $(v_c^i, v_w^i) \in [0.1, 0.9]^2$. In Fig. 7, the mean value of the average cellular datarate increases with an increase in the ratio. This implies that as the entity gives more preference to its cellular network, its performance improves. An interesting trend is observed for the WiFi datarates. After a dip at $\theta_c = 2\theta_w$, it rises back up $\theta_c = 5\theta_w$ onwards.

In Fig. 5, we observed that the average cellular datarate without using the unlicensed band ($\delta_c = 0$), is $\sim$ 40 Mbps. Similarly, the average WiFi datarate without utilizing the unlicensed band ($\delta_w = 0$) is $\sim$ 50 Mbps. Comparing these values with the maximum value of the average datarate observed in Fig. 7 for $\theta_c = 6\theta_w$, we see up to 44% and 340% improvements in cellular and WiFi datarates, respectively.

In Fig. 8, for the same entities playing the same game, the Nash equilibrium changes due to difference in the value of the ratio $\frac{\theta_c}{\theta_w}$. In Fig. 8a, we give 7 times more preference to the cellular network datarate compared to its WiFi counterpart, due to which the cellular datarate of both entities settle at $\sim$ 55 Mbps which satisfies the datarate requirement of both the entities. Moreover, the equilibrium is satisfactory for both networks of each entity. In contrast, in Fig. 8b where $\theta_c = 5\theta_w$ we observe that the datarate requirements of entity-1 are not met at all. This could be attributed to entity-2 greedily setting δ_w^2 value to 1 to maximize its WiFi datarate. In the subsequent iterations, none of the actions by entity-1 could satisfy its datarates, so it saturates at $\delta_c^1 = 0, \delta_w^1 = 0$. Therefore tuning the value of the ratio $\frac{\theta_c}{\theta_w}$ is essential for system performance.

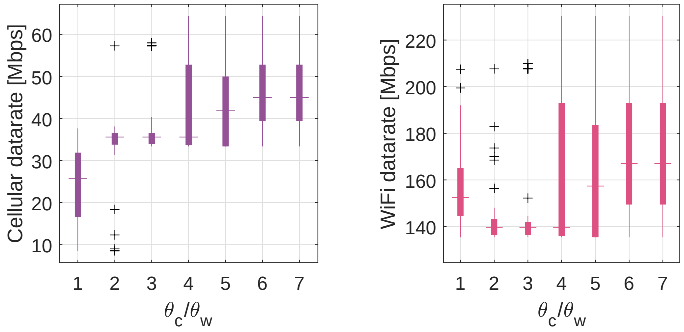

Fig. 7: Average cellular and WiFi datarates at Equilibrium for different values of θ_c/θ_w. $|\mathcal{E}| = 2$.

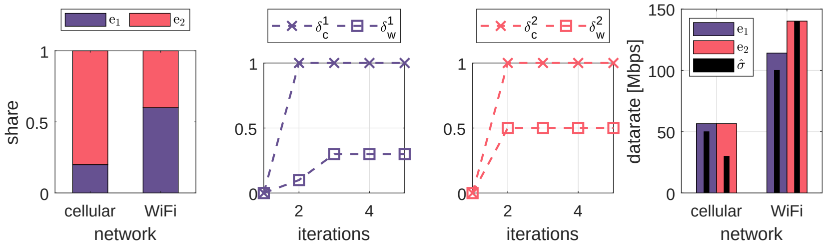

(a) $\theta_c = 7\theta_w$

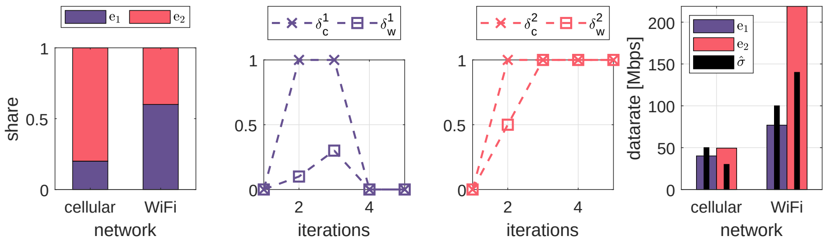

(b) $\theta_c = 5\theta_w$

Fig. 8: Nash Equilibria due to difference in θ_c/θ_w. $|\mathcal{E}| = 2$.

B. *Effect of Datarate Thresholds*

We study two entities with identical datarate requirements and vary $(v_c^1, v_w^1) \in [0.1, 0.9]^2$. Then, we analyse the empirical *complementary cumulative density function* (CCDF) of the cellular and WiFi datarates for different values of minimum cellular and WiFi datarate thresholds. The value of this CCDF at x, is referred to as the *rate coverage probability* (RCP) at datarate threshold equal to x. We also determine the mean of the average datarates with respect to the different values of network shares (v_c^1, v_w^1).

We first comment on the variation in average cellular datarate due to different datarate thresholds as shown in Fig. 9 and we observe the following:

- The datarate requirement is perfectly met when the WiFi datarate threshold $\hat{\sigma}_w$ is low (100 Mbps) as well as the cellular datarate threshold $\hat{\sigma}_c$ is low (30 Mbps).
- Setting the cellular datarate threshold to a value higher than the true requirement ensures a higher rate coverage probability (RCP) at the true requirement. For example, when $\hat{\sigma}_c = 50$ Mbps and $\hat{\sigma}_w = 150$ Mbps, the RCP at 50 Mbps is ~ 0.2, but it shoots up to ~ 0.9 at 30 Mbps.
- The RCP decreases with increase in the WiFi datarate threshold $\hat{\sigma}_w$. The only anomaly to this trend being the curve for $\hat{\sigma}_c = 30$ Mbps and $\hat{\sigma}_w = 150$ Mbps.

Next, we comment on the variation in the average WiFi datarate due to datarate thresholds. The rate coverage probability of average WiFi datarate is presented in Fig. 10, based on which we make the following observations:

- The rate coverage probability is 1 when the WiFi datarate threshold is low, i.e., $\hat{\sigma}_w = 100$ Mbps.
- For the same cellular datarate threshold $\hat{\sigma}_c$, the RCP increases on increasing the WiFi datarate threshold $\hat{\sigma}_w$.
- The RCP decreases as the cellular datarate threshold $\hat{\sigma}_c$ is increased.

The only curve which does not abide by these trends is $\hat{\sigma}_c = 30$ Mbps, $\hat{\sigma}_w = 150$ Mbps.

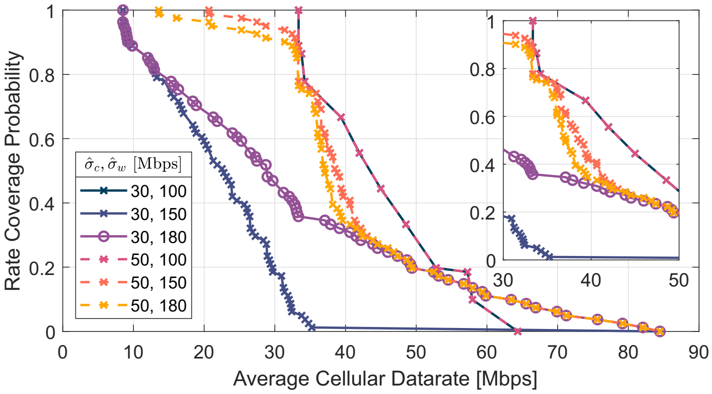

Fig. 9: Empirical CCDF of average cellular datarate. Parameters: $|\mathcal{E}| = 2$, $\theta_c/\theta_w = 7$.

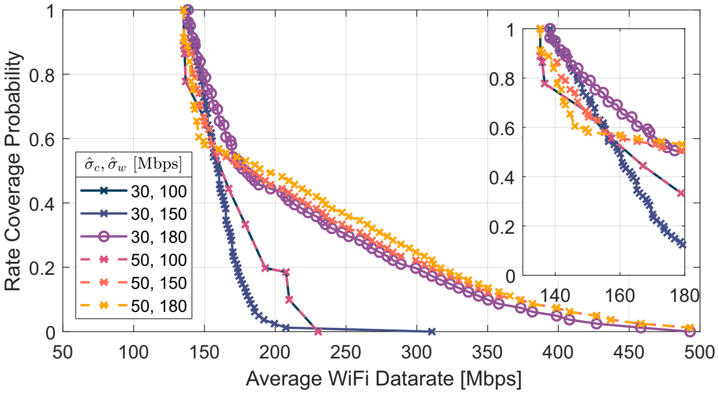

Fig. 10: Empirical CCDF of average WiFi datarate. Parameters: $|\mathcal{E}| = 2$, $\theta_c/\theta_w = 7$.

In Fig. 11a, we can see that for $\hat{\sigma}_c = 50$ Mbps, the mean of the average cellular datarate decreases with increase in the WiFi datarate threshold $\hat{\sigma}_w$. Similarly in Fig. 11b, we see the mean of the average WiFi datarate increasing with increase in the WiFi datarate threshold $\hat{\sigma}_w$. In summary, the values of $\hat{\sigma}_c$ and $\hat{\sigma}_w$ should be chosen carefully by the entity based on its true requirements.

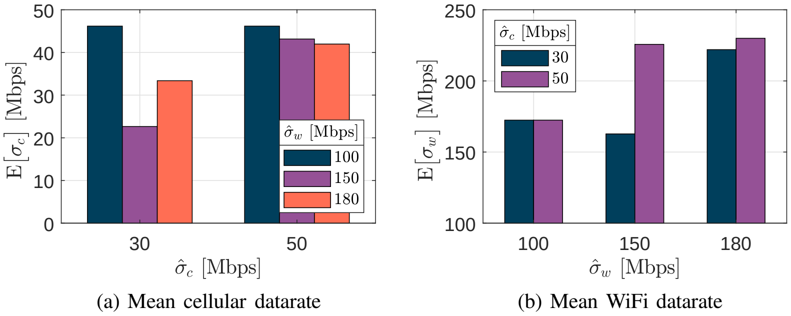

(a) Mean cellular datarate

(b) Mean WiFi datarate

Fig. 11: Mean of the average cellular and WiFi datarate for various values of datarate thresholds, $|\mathcal{E}| = 2$, $\theta_c/\theta_w = 7$.

C. *Effect of Network Share*

In the interaction of two entities, where entity e_1's cellular network share is v_c^1 and its WiFi network share is v_w^1, we record the datarates achieved by its networks at equilibrium for different values of the tuple (v_c^1, v_w^1). We consider the two entities to have the same datarate thresholds, therefore presenting the results for the first entity is sufficient. In essence, we analyse the trends for the following scatter plots: (i) σ_w^1 vs. v_w^1 (Fig. 12), and (ii) σ_c^1 vs. v_c^1 (Fig. 13).

In Fig. 12, we observe that the average WiFi datarate tends to decrease as the WiFi share of that entity increases. This trend is strongly linear for $\hat{\sigma}_w = 100$ Mbps. The blue markers are the datarate values for different values of (v_c^1, v_w^1) and we plot a linear fit in red.

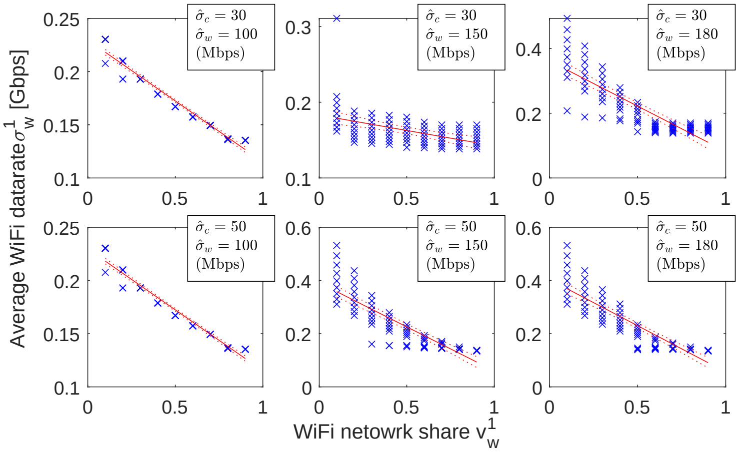

Fig. 12: Effect of WiFi network share on WiFi datarate.

Now, we see how an entity's share of cellular network v_c^1 affects its average cellular datarate. In Fig. 13, we see that the cellular network share does not affect the cellular datarate when the WiFi datarate threshold is 100 Mbps. However, we see that the cellular datarate increases with increase in cellular network share for $\hat{\sigma}_w \in \{150, 180\}$ Mbps.

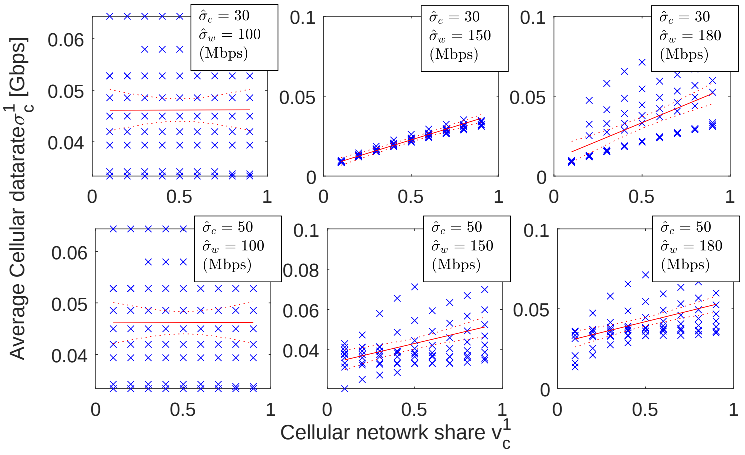

Fig. 13: Effect of cellular network share on cellular datarate.

Furthermore, as we compare Fig. 12 with Fig. 13, we see that if the entity has a higher WiFi share, its WiFi datarate is lower and if the entity has a higher cellular share, its cellular datarate is higher. This anomalous relationship between the two RATs' network share on its corresponding network's datarate is interesting. Inspection of theorems 1 and 2 reveals that the relation between the datarates and network shares is not analytically straightforward, as it depends on the values of δ_c^i, δ_w^i at equilibrium, which in turn depends on other system parameters.

D. Cellular vs. WiFi

We consider a special case, where one entity owns the cellular network entirely and the other entity owns the complete WiFi network. In Fig. 14, the datarate requirements of both entities are satisfied at equilibrium. The cellular network in both cases, settles at $\delta_c^1 = 1$, while the WiFi network settles at $\delta_w^2 \approx 0.4$ when $\hat{\sigma}_w^2 = 120$ Mbps in Fig. 14a and at $\delta_w^2 \approx 0.5$ when $\hat{\sigma}_w^2 = 130$ Mbps in Fig. 14b. Due to the increase in WiFi datarate threshold, the cellular datarate decreases in Fig. 14b, even though the minimum cellular datarate requirement is still met.

E. Three-Entity Game

Next, we demonstrate that our framework works for more than two entities. Here three entities owning different shares of the cellular and WiFi networks interact such that the minimum datarate requirement of each entity is met at equilibrium.

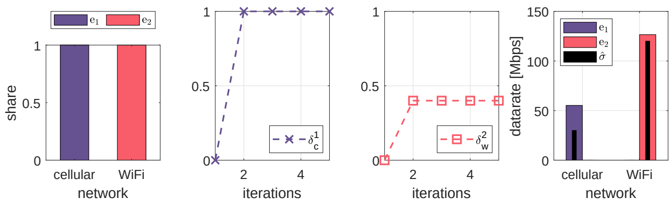

(a) $\hat{\sigma}^1_c = 30$ Mbps, $\hat{\sigma}^2_w = 120$ Mbps.

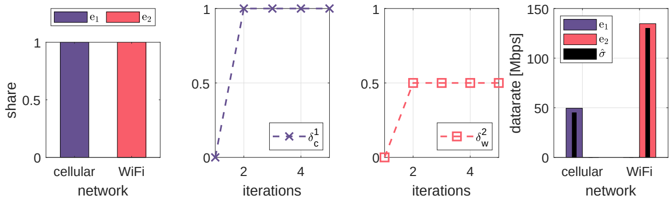

(b) $\hat{\sigma}^1_c = 45$ Mbps, $\hat{\sigma}^2_w = 130$ Mbps.

Fig. 14: Interaction of two entities when one entity is entirely cellular and the other is entirely WiFi: $v^1_c = 1$, $v^2_w = 1$. Parameters: $|\mathcal{E}| = 2$, $\theta_c = 7\theta_w$.

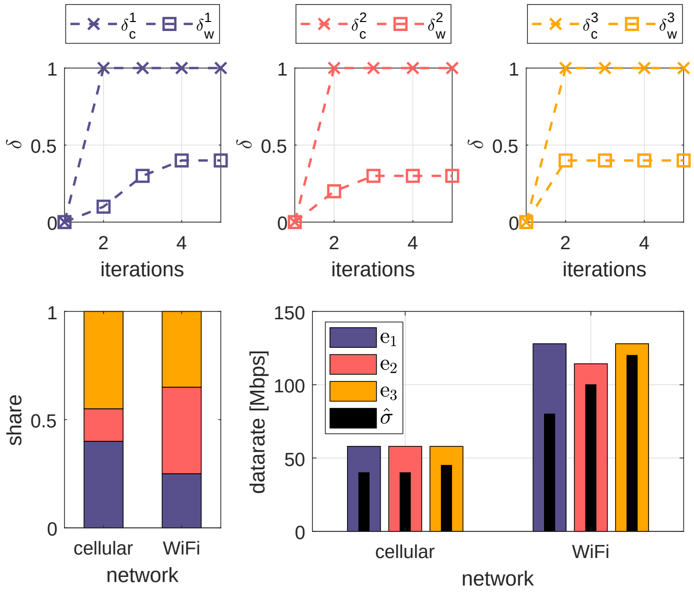

Fig. 15: Exemplary three-entity interaction, $\theta_c = 7\theta_w$.

In Fig. 15, the cellular and WiFi datarate thresholds are crossed by each entity. It must be noted that the entities have their WiFi datarate inversely proportional to the WiFi network share. This trend was supported in our analysis of two-entity interaction, earlier in this section (see Fig. 12).

VI. CONCLUSION

In this work, we provided a game-theoretic framework for analyzing the interaction between different networks, namely, cellular, WiFi or a combination of both, as they utilize the unlicensed spectrum in addition to their licensed spectra, in the presence of incumbent users. We have shown how the system parameters affect the performance of a network at equilibrium and quantified the throughput gains of the networks as a result of using the 6 GHz bands, which offer larger bandwidths. The proposed framework is flexible and can be used to model a variety of scenarios for feasibility and performance assessment of the networks involved.

In this work, we have considered a stochastic setup and focused on a large-scale network. One possible extension to this work is to consider deterministic setups with the aim of optimizing spectrum selection among the two RATs for a given set of locations.

APPENDIX A
LAPLACE TRANSFORMS

The Laplace transform of the interference [23] experienced by the cellular users in the unlicensed band from transmitters of type $j \in \{c, w, z\}$ is mathematically express as $\mathcal{L}_{c,j|U}(s)$:

$$\begin{aligned}\mathcal{L}_{c,j|U}(s) &\overset{j\neq c}{=} \exp\left(-\pi\lambda_{j|U}\frac{(s\,p_j)^{\frac{2}{\alpha}}}{\mathrm{sinc}\left(\frac{2}{\alpha}\right)}\right),\\ &\overset{j=c}{=} \exp\left(-\int_r^\infty \frac{2\pi\lambda_{c|U}}{1+(s\,p_c)^{-1}x^\alpha}\,x\,dx\right).\end{aligned}$$

Similarly, the Laplace transform of the interference experienced by the WiFi users in the unlicensed band from the transmitters of type $j \in \{c, w, z\}$ is mathematically express as $\mathcal{L}_{w,j|U}(s)$:

$$\mathcal{L}_{w,j|U}(s) = \exp\left(-\pi\lambda_{j|U}\frac{(s\,p_j)^{\frac{2}{\alpha}}}{\mathrm{sinc}\left(\frac{2}{\alpha}\right)}\right).$$

REFERENCES

[1] FCC. (2020, Apr.) *Report and Order and Further Notice of Pro- posed Rulemaking; In the Matter of Unlicensed Use of the 6 GHz Band (ET Docket No. 18-295); Expanding Flexible Use in Mid- Band Spectrum Between 3.7 and 24 GHz (GN Docket No. 17-183).* Available online: https://docs.fcc.gov/public/attachments/FCC-20-51A1.pdf.

[2] Fixed Wireless Communications Coalition. (2019, Jul.) *Deploying 6 GHz RLANs While Protecting the Fixed Service. Comments to the FCC GN*. Docket nos. 17-183. Available online: https://bit.ly/3odu4b3.

[3] Wireless Innovation Forum. (2019, Dec.) *Propagation Models and Interference Protection Criteria for Sharing between the Fixed Service and Unlicensed Devices in the 6GHz Band*. Document WINNF-TR-1002, Version V1.0.0.

[4] E. J. Sacoto Cabrera, L. Guijarro, and P. Maillé, "Game Theoretical Analysis of a Multi-MNO MVNO Business Model in 5G Networks," *Electronics*, vol. 9, no. 6, p. 933, 2020.

[5] G. Naik, *et al.*, "Next generation Wi-Fi and 5G NR-U in the 6 GHz bands: Opportunities and challenges," *IEEE Access*, vol. 8, pp. 153 027–153 056, 2020.

[6] E. J. Oughton, *et al.*, "Revisiting wireless internet connectivity: 5G vs Wi-Fi 6," *arXiv preprint arXiv:2010.11601*, 2020.

[7] WBA NGMN Alliance. (2019, Sep.) *Joint NGMN/WBA RAN Convergence Paper*. Available online: https://www.ngmn.org/publications/joint-ngmn-wba-ran-convergence-paper.html.

[8] V. Sathya, *et al.*, "Standardization Advances for Cellular and Wi-Fi Coexistence in the Unlicensed 5 and 6 GHz Bands," *GetMobile: Mobile Computing and Communications*, vol. 24, no. 1, pp. 5–15, 2020.

[9] G. Naik, J. Liu, and J.-M. J. Park, "Coexistence of wireless technologies in the 5 GHz bands: A survey of existing solutions and a roadmap for future research," *IEEE Communications Surveys & Tutorials*, vol. 20, no. 3, pp. 1777–1798, 2018.

[10] C. Cano and D. J. Leith, "Unlicensed LTE/WiFi coexistence: Is LBT inherently fairer than CSAT?" in *2016 IEEE International Conference on Communications (ICC)*, 2016, pp. 1–6.

[11] M. Mehrnoush, *et al.*, "On the fairness of Wi-Fi and LTE-LAA coexistence," *IEEE Transactions on Cognitive Communications and Networking*, vol. 4, no. 4, pp. 735–748, 2018.

[12] S. Lagen, *et al.*, "New radio beam-based access to unlicensed spectrum: Design challenges and solutions," *IEEE Communications Surveys & Tutorials*, vol. 22, no. 1, pp. 8–37, 2019.

[13] P. C. Pinto, *et al.*, "A stochastic geometry approach to coexistence in heterogeneous wireless networks," *IEEE Journal on Selected Areas in Communications*, vol. 27, no. 7, pp. 1268–1282, 2009.

[14] A. Bhorkar, C. Ibars, and P. Zong, "Performance analysis of LTE and Wi-Fi in unlicensed band using stochastic geometry," in *2014 IEEE 25th Annual International Symposium on Personal, Indoor, and Mobile Radio Communication (PIMRC)*, 2014, pp. 1310–1314.

[15] A. M. Voicu, L. Simić, and M. Petrova, "Inter-technology coexistence in a spectrum commons: A case study of Wi-Fi and LTE in the 5-GHz unlicensed band," *IEEE Journal on Selected Areas in Communications*, vol. 34, no. 11, pp. 3062–3077, 2016.

[16] Y. Wu, *et al.*, "Repeated open spectrum sharing game with cheat-proof strategies," *IEEE Transactions on Wireless Communications*, vol. 8, no. 4, pp. 1922–1933, 2009.

[17] B. Wang, *et al.*, "Game theoretical mechanism design methods," *IEEE Signal Processing Magazine*, vol. 25, no. 6, pp. 74–84, 2008.

[18] F. Teng, D. Guo, and M. L. Honig, "Sharing of unlicensed spectrum by strategic operators," *IEEE Journal on Selected Areas in Communications*, vol. 35, no. 3, pp. 668–679, 2017.

[19] C. Hasan, M. K. Marina, and U. Challita, "On LTE-WiFi coexistence and inter-operator spectrum sharing in unlicensed bands: Altruism, cooperation and fairness," ser. MobiHoc '16. New York, NY, USA: Association for Computing Machinery, 2016, p. 111–120.

[20] M. A. Kishk and H. S. Dhillon, "Tight Lower Bounds on the Contact Distance Distribution in Poisson Hole Process," *IEEE Wireless Communications Letters*, vol. 6, no. 4, pp. 454–457, 2017.

[21] ——, "Coexistence of rf-powered iot and a primary wireless network with secrecy guard zones," *IEEE Transactions on Wireless Communications*, vol. 17, no. 3, pp. 1460–1473, 2017.

[22] A. M. Hayajneh, *et al.*, "Performance analysis of uav enabled disaster recovery networks: A stochastic geometric framework based on cluster processes," *IEEE Access*, vol. 6, pp. 26 215–26 230, 2018.

[23] B. Blaszczyszyn, *et al.*, *Stochastic Geometry Analysis of Cellular Networks*. Cambridge University Press, 2018.

[24] S. Durand, F. Garin, and B. Gaujal, "Distributed best response algorithms for potential games," in *2018 European Control Conference (ECC)*, 2018, pp. 2170–2175.

[25] 3GPP, "NR; User Equipment (UE) Radio Transmission and Reception; Part 1: Range 1 Standalone," 3rd Generation Partnership Project, Technical Specification (TS) 38.101-1, 07 2020, release 16.4.0. [Online]. Available: https://www.3gpp.org/DynaReport/38101-1.htm

[26] D. López-Pérez, *et al.*, "Ieee 802.11be extremely high throughput: The next generation of Wi-Fi technology beyond 802.11ax," *IEEE Communications Magazine*, vol. 57, no. 9, pp. 113–119, 2019.

[27] I. T. Union, *Handbook on Land Mobile (including Wireless Access)*, 2nd ed. International Telecommunication Union, vol. 1.

[28] A. Weissberger. (2020, Aug.) *5G Base Station Deployments; Open-RAN Competition & HUGE 5G BS Power Problem*. Available online: https://techblog.comsoc.org/2020/08/07/5g-base-station-deployments-open-ran-competition-huge-5g-bs-power-problem/.

[29] M. Ding, *et al.*, "On the fundamental characteristics of ultra-dense small cell networks," *IEEE Network*, vol. 32, no. 3, pp. 92–100, 2018.

[30] K. Jones and L. Liu, “What where Wi: An analysis of millions of Wi-Fi access points,” in *2007 IEEE International Conference on Portable Information Devices*. IEEE, 2007, pp. 1–4.

[31] C. Sun and R. Jiao, “Discrete exclusion zone for dynamic spectrum access wireless networks,” *IEEE Access*, vol. 8, pp. 49 551–49 561, 2020.